313

Effect of benzotriazole on the electrochemical behaviour of cadmium in alkaline solutions

S. Tamil Selvan*, R. Sabapathi and **N. Venkatakrishnan**
Central Electrochemical Research Institute, Karaikudi 623 006 (India)

Abstract

Modification of the electrochemical behaviour of the cadmium electrode by benzotriazole (BTA) has been extensively studied by potentiodynamic experiments. BTA is found to react with metallic cadmium to form surface films that provide large electrochemically active surface areas. A complexation phenomenon, as detected by IR spectra, is suggested.

Introduction

At present, there is considerable interest in the effect of organic compounds on the capacity of the cadmium electrode in sintered-plate Ni/Cd batteries. Two different mechanisms have been proposed, namely, a solid-state growth mechanism [1, 2], and a dissolution–precipitation mechanism [3–9] where soluble intermediates (such as $Cd(OH)_3^-$ and $Cd(OH)_4^{2-}$) play a role in the charge/discharge reaction. The latter mechanism has been shown to be predominant in KOH solutions of concentration greater than 1 M. Sintered-plate cadmium inefficiencies have been attributed to re-distribution and crystal size changes of the active material [10–12].

The inclusion of 20 wt.% Fe into the active material during impregnation yields better capacity output at both high and low rates of discharge [13]. The behaviour of additives (viz., carboxymethyl cellulose [14] and polyvinyl alcohol [15]) at the planar $Cd/Cd(OH)_2$ electrode interface is well documented. More recently, it has been observed that BTA minimizes the decline in capacity of sintered cadmium electrodes during the initial stages of cycling [16]. Nevertheless, much is unknown about the action of BTA. The present paper reports potentiodynamic studies of the behaviour of planar cadmium electrodes in the active dissolution region in the presence of BTA.

Experimental

Apparatus

Cyclic voltammetry was performed using a Wenking potentiostat (Model ST 72) in conjunction with a voltage scan generator (Model VSG 72).

---

*Author to whom correspondence should be addressed.

Voltammograms were recorded using a Rikadenki X–Y recorder. Measurements were made in a conventional, enclosed 'H'-type cell with a counter electrode made from nickel foil of large area. All potentials are reported with regard to an Hg/HgO/5 M KOH reference electrode.

Reagents and materials

Analytical Reagent grade BTA and KOH were used. The solution was 5 M KOH prepared from triply-distilled water.

The cadmium electrode was in the form of a disc of area 0.20 cm². This was cut from a rod supplied by BDH (99.9% pure) and was set in an Araldite holder.

Procedure

Prior to experiment, the cadmium electrode was mechanically polished with 4/0 emery paper wetted with methanol, cleaned with methanol and water, and then polished with 1 μm diamond paste. Subsequent polishing was carried out on a buff (particle size 1 μm). The electrode was rinsed with methanol and water before immersion in the working solution.

Oxygen was removed from the test solution prior to experiment by bubbling pre-purified nitrogen through the cell. The basic voltammetric sweep rate used in this work was 20 mV s^{-1}, although other sweep rates were applied in certain cases to obtain a qualitative estimate of any variation in electrode behaviour related to a change in sweep rate.

Results and discussion

Cyclic voltammetry of cadmium in 5 M KOH

In KOH alone, a cadmium electrode gave the voltammogram shown in Fig. 1 over the potential range −1.2 to −0.7 V. It can be seen that the oxidation current increases sharply at potentials less negative than about −0.9 V. This anodic reaction is due to the oxidation of Cd to Cd(II) in the form of soluble species, viz., $Cd(OH)_3^-$ and $Cd(OH)_4^{2-}$. The former has been shown [17] to be the predominant species at a potential of −0.887 V; beyond this, precipitation of $Cd(OH)_2$ results. The single anodic peak at −0.860 V relates to the active dissolution of cadmium followed by passivation. Good evidence for the presence of a film at this potential has been obtained [18] from low-frequency impedance measurements. After the first cathodic peak, a considerable amount of unreduced hydroxide remains and this explains the reduced anodic peak height on the subsequent anodic scan. The imbalance between charge and discharge decreases with further cycling. The anodic peak diminishes on cycling and, after 30 cycles, the peak has been displaced 10 mV negative to the original peak. This demonstrates the inefficiency of the cadmium electrode. Continuous cycling gives a constant peak current after 50 cycles.
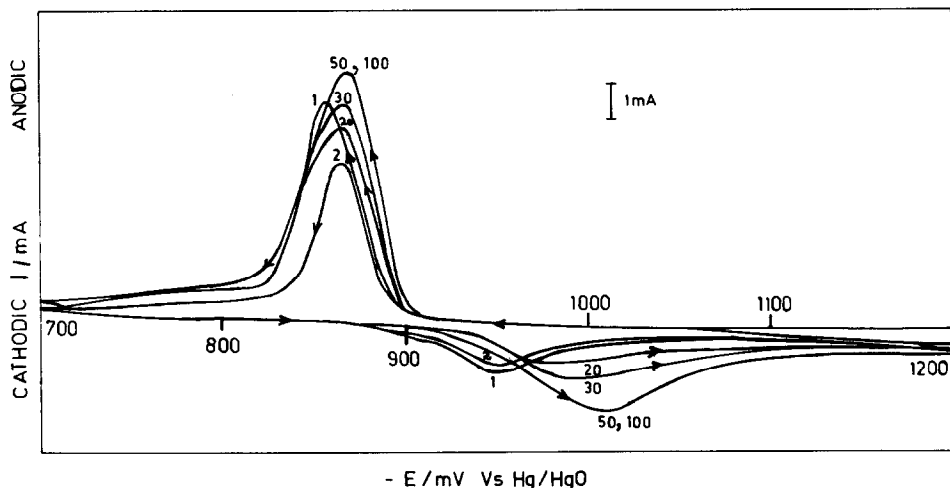
Fig. 1. Cyclic voltammograms for cadmium in 5 M KOH. Scan rate: 20 mV s^{-1}. Cycle numbers as indicated.
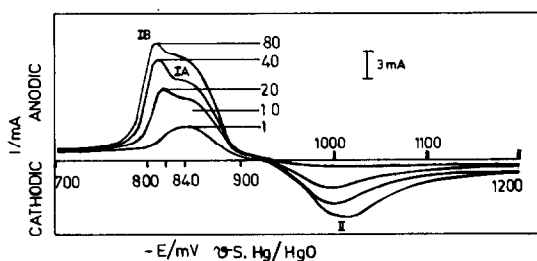

Fig. 2. Cyclic voltammograms for cadmium in 5 M KOH containing 0.01 M BTA. Scan rate: 20 mV s^{-1}. Cycle numbers as indicated.

Cyclic voltammetry of cadmium in presence of BTA

The cyclic voltammogram obtained for cadmium in a 5 M KOH solution containing 0.01 M BTA is given in Fig. 2. The first sweep produces a trace consisting of well-defined oxidation and reduction peaks at −0.850 and −1.0 V, respectively. Successive cycling (after about 5 cycles) introduces a new peak, IA, at −0.845 V.

The product associated with peaks IA and IB is claimed to be Cd(II)−BTA and Cd(OH)$_2$, respectively. It is found that the peak current at IA and IB increases linearly with the square root of the potential sweep rate, indicating that the reaction is controlled by a diffusion process in the oxide phase.

The addition of BTA to the electrolyte causes a marked change in the polarization curve. Initially, the anodic peak height diminishes due to unreduced Cd(OH)$_2$. After 3 cycles, however, the peak height begins to increase; this may reflect the probable adsorption of BTA. The cyclic voltammetric behaviour observed may be explained in terms of the known dependence of the adsorption of organic molecules upon electrode charge [19–21].

The shift in peak potential, and the increase in peak height, are both thought to be due to roughening of the surface by the deposition of finely divided cadmium during Cd(II)–BTA reduction. The finely divided cadmium, which has a large surface area, is oxidized more readily than a freshly polished cadmium surface, i.e., peak IA occurs at a more negative potential. Further, roughening increases the efficiency of the cadmium electrode, as shown by the peak being displaced 20 mV positive to the original peak. Therefore, after about 80 cycles (Fig. 2), a greater amount of charge is required in the oxidative process to passivate the electrode surface.

Sweep-rate dependence

The principal aim of the present study was to obtain quantitative data on the sweep-rate dependence of the oxidation/reduction behaviour of the cadmium electrode in KOH solution containing BTA.

An increase in the sweep rate was found to displace peaks I and II to more noble and active potentials, respectively. On the other hand, the characteristics of peak IA are only slightly dependent upon sweep rate (Fig. 3). It cannot be clearly distinguished in every sweep rate. Thus, it is concluded that BTA requires that some sort of energy be adsorbed onto the surface of the cadmium electrode.

Peak potentials (E_p) and currents (i_p) were recorded over a range of sweep rates (v) from 1 to 200 mV s^{-1}. They are respectively plotted as a function of $v^{1/2}$ in Figs. 4 and 5.

Figure 6 presents the potentiodynamic curves for a cadmium electrode in 5 M KOH containing 0.1 M BTA. The dependence of i_p^a and i_p^c on BTA strength in 5 M KOH is shown in Table 1. In general, traces obtained at very low sweep rates exhibit only one defined oxidation peak on the positive-
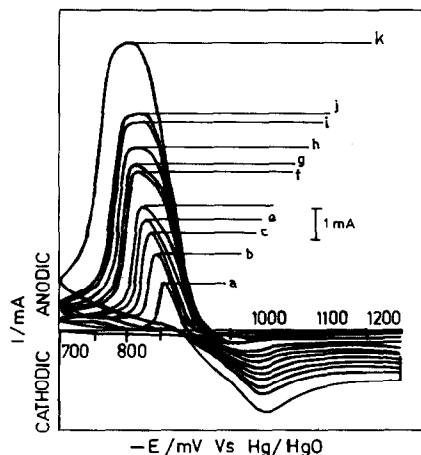

Fig. 3. Cyclic voltammograms for a fresh cadmium electrode in 5 M KOH containing 0.01 M BTA at different scan rates: (a) 10, (b) 20, (c) 30, (d) 40, (e) 50, (f) 60, (g) 70, (h) 80, (i) 90, (j) 100, (k) 200 mV s^{-1}.
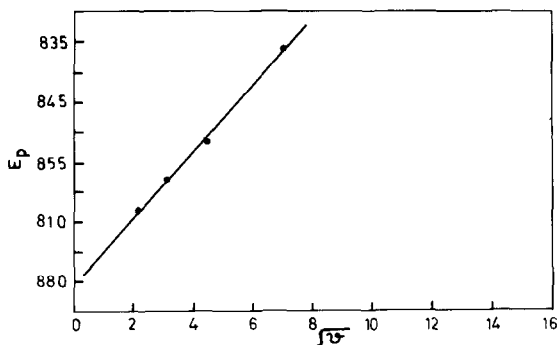
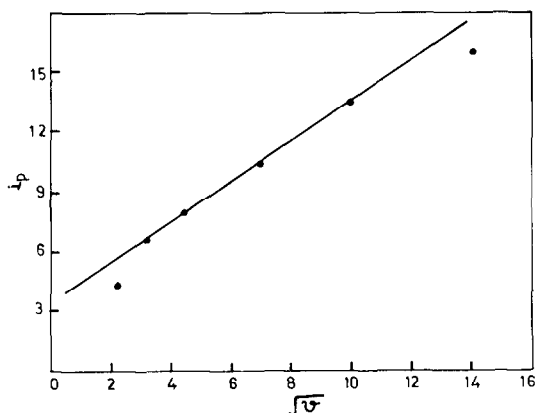Fig. 4. E_p vs. $v^{1/2}$ plot for cadmium in 5 M KOH containing 0.01 M BTA.

Fig. 5. i_p vs. $v^{1/2}$ plot for cadmium in 5 M KOH containing 0.01 M BTA.
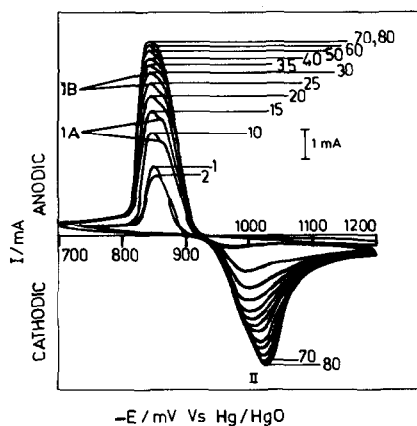

Fig. 6. Cyclic voltammograms for cadmium in 5 M KOH containing 0.1 M BTA. Cycle numbers as indicated.

TABLE 1

Dependence of i_p^a and i_p^c (after cycling, e.g., 80th cycle) on BTA strength in 5 M KOH

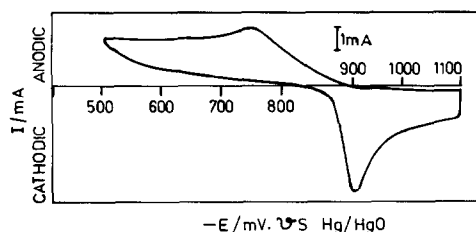| Molarity of BTA	i_p^a (mA)	i_p^c (mA)
0.0	6.8	3.25
0.01	12	6.0
0.1	6.1	4.0
1.0	2.0	3.5

Fig. 7. Cyclic voltammograms for a fresh cadmium electrode in 5 M KOH containing 1 M BTA.

going sweep, and one reduction peak on the reverse sweep. Continuous cycling results in the introduction of a new peak (IA). Therefore, it is again well established that adsorption of BTA onto the cadmium electrode requires some sort of energy. At higher sweep rates, peak IA is not well defined, thereby preventing the acquisition of quantitative data for peak potentials and currents.

When the BTA concentration was raised to 1 M, the voltammogram shown in Fig. 7 was obtained. It is apparent that the peak has decreased somewhat in size and shifted to a more positive potential. The main effect of increased BTA concentration is to enhance the dissolution of cadmium which now occurs near -0.82 V.

Sweep reversal studies

In order to define the origins of the reduction peaks subsequent to anodic oxidation, a number of sweep reversal experiments were performed. If the positive-going sweep is reversed, only one reduction peak is observed; there is no reduction peak corresponding to peak IA. Reversal of the forward sweep at potentials more positive than those of peaks IA and IB gives rise to only one reduction peak (Fig. 7). The same holds true when the forward sweep is reversed at potentials more negative than those of peaks IA and IB. Therefore, it can be concluded that the reduction of both Cd(II)–BTA and $Cd(OH)_2$ takes place simultaneously.
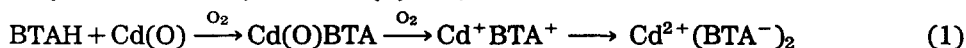
IR spectra

The infrared (IR) spectrum of BTA is shown in Fig. 8. This displays an N–H stretching absorption frequency in the region 3400–2200 cm^{-1}. BTA contains three nitrogen atoms: two are so-called pyridine nitrogens, the other is a pyrrole nitrogen. In the solid state, the imino group of BTA forms different kinds of hydrogen bonding (N–H...N) with the pyridine nitrogen, giving rise to strong multiple absorption in the region 3300–2300 cm^{-1}.

The infrared spectrum of the electroactive material (Cd + BTA) obtained [16] for sintered plate cadmium showed the complete absence of the N–H stretching absorption frequency in the region 3400–2200 cm^{-1} and the N–H bending absorption in the region 1500–1250 cm^{-1}. This indicates de-protonation of the chemisorbed BTAH (Fig. 9). Therefore, it is suggested that BTA is present in the form of the de-protonated anion (BTA$^-$).

The electrode reaction corresponding to peak IA is clearly the formation of a solid on the electrode surface. Visual inspection of the electrode showed that after peak IA, the surface was covered with a light brown layer. An IR spectra of this surface film indicated that, within the limits of this technique, only bis(benzotriazolato)Cd(II) was present.

We propose that BTA forms a ligand to the cadmium atom to produce a Cd(I)BTA complex. The latter is then oxidized and de-protonated to yield bis(benzotriazolato)cadmium(II) i.e.,

$$BTAH + Cd(O) \xrightarrow{O_2} Cd(O)BTA \xrightarrow{O_2} Cd^+BTA^+ \longrightarrow Cd^{2+}(BTA^-)_2 \qquad (1)$$

In fact, it has been reported [22] that imidazolato–metal(I) is a polymeric material. Reference has also been made [23] to X-ray crystallographic evidence
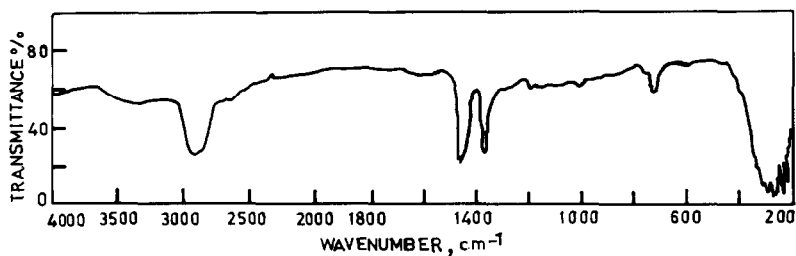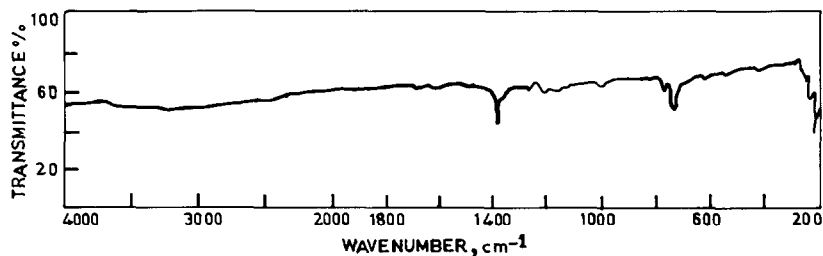

Fig. 8. IR spectrum of BTA.

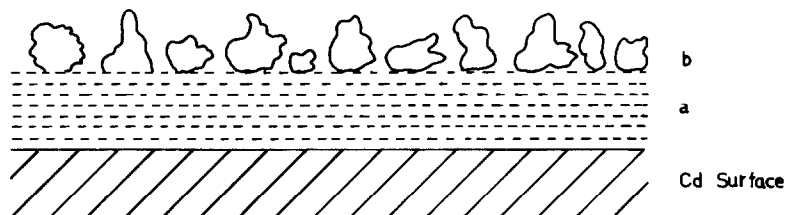Fig. 9. IR spectrum of cadmium with BTA.

Fig. 10. Schematic of anodic formation of different layers of cadmium complex: (a) compact layer; (b) loose layer.

that indicates bis(imidazolato)zinc to be polymeric. Therefore, we suggest that the polymer film covering the surface of the cadmium electrode enhances the electrochemically-active surface areas.

Structure of complex layers

The layer of bis-(benzotriazolato)cadmium(II) that forms on the cadmium surface when the potential is increased to -0.7 V is compact and adherent. If the potential is held at -1.2 V for some time, or increased beyond -0.8 V, and the electrode surface is examined under a microscope, different layers of cadmium complex can be observed, Fig. 10.

Possibly, the compact layer of cadmium complex reduces more readily (at a less negative potential) because it is in good electrical contact with the underlying metal. The thickness of the compact layer is essentially independent of sweep rate as demonstrated by the fact that the charge passed during the tracing of peak IA is the same for all sweep rates. In contrast to the compact layer, the powdery layer grows to a much greater average thickness at higher sweep rates. This can be seen from the magnitude of the residual current flowing after the formation of the passive layer. After cycling for some time, peak IB grows at the expense of peak IA. The cadmium surface becomes roughened during cycling and its ability to form a flaw-free compact layer is progressively reduced.

Acknowledgements

References

1 G. T. Croft, *J. Electrochem. Soc.*, *106* (1959) 278.
2 R. D. Armstrong and G. D. West, *J. Electroanal. Chem.*, *30* (1971) 385.
3 P. E. Lake and E. J. Casey, *J. Electrochem. Soc.*, *105* (1958) 52.

4 P. E. Lake and E. J. Casey, *J. Elecrochem. Soc.*, *106* (1959) 913.

5 S. Yoshizawa and Z. Takehara, *Electrochim. Acta.*, *5* (1961) 240.

6 M. W. Breiter and J. L. Weininger, *J. Electrochem. Soc.*, *113* (1966) 651.

7 M. W. Breiter and W. Vedder, *Trans. Faraday Soc.*, *63* (1967) 1042.

8 M. A. V. Devanathan and S. Lakshmanan, *Electrochim. Acta.*, *13* (1968) 667.

9 Y. Okinaka, *J. Electrochem. Soc.*, *117* (1970) 289.

10 J. L. Weininger and M. W. Breiter, in D. H. Collins (ed.), *Power Sources*, Pergammon Press, 1967, pp. 269–286.

11 P. Bro and H. Y. Kang, *J. Electrochem. Soc.*, *117* (1971) 583.

12 A. J. Salkind, H. J. Canning and M. L. Block, *J. Electrochem. Soc.*, *2* (1964) 254.

13 S. Tamil Selvan, S. Nathira Begum, VR. Chidambaram, R. Sabapathi and K. I. Vasu, *J. Power Sources*, *32* (1990) 55.

14 S. Tamil Selvan, R. Sabapathi and N. Venkatakrishnan, *Bull. Electrochem.*, *6* (1990) 266.

15 M. Z. A. Munshi, A. C. C. Tseung and D. Misale, *J. Power Sources.*, *23* (1988) 341.

16 S. Tamil Selvan, R. Sabapathi and N. Venkatakrishnan, *J. Appl. Electrochem.*, in press.

17 F. G. Will, *J. Electrochem. Soc.*, *136* (1989) 2194.

18 R. D. Armstrong and K. Edmondson, *J. Electroanal. Chem.*, *53* (1974) 371.

19 J. O. M. Bockris and A. K. N. Reddy, *Modern Electrochemistry*, Vol. 2, Plenum Press, New York, 1970, p. 793.

20 E. Gileadi, *J. Electroanal. Chem.*, *11* (1966) 137.

21 E. Gileadi and K. Muller, *Electrochim. Acta*, *12* (1967) 1301.

22 G. P. Brown and S. A. Aftergut, *J. Polym. Sci.*, Part A, *2* (1964) 1839.

23 M. Goodgame and F. A. Cotton, *J. Am. Chem. Soc.*, *84* (1962) 1543.